THE ASTROPHYSICAL JOURNAL, 556:373–379, 2001 July 20

INFRARED OBSERVATIONS AND MODELING OF ONE OF THE COOLEST T DWARFS: GLIESE 570D

T. R. GEBALLE,[1] D. SAUMON,[2] S. K. LEGGETT,[3] G. R. KNAPP,[4] M. S. MARLEY,[5] AND K. LODDERS[6]

Received 2001 February 12; accepted 2001 March 8

ABSTRACT

We have obtained a good-quality $R \sim 400$, 0.8–2.5 μm spectrum as well as accurate photometry of Gliese 570D, one of the coolest and least-luminous brown dwarfs currently known. The spectrum shows that Gl 570D has deeper absorptions in the strong water and methane bands at 1.12–1.17, 1.33–1.45, 1.62–1.88, and 2.20–2.45 μm and is both bluer at $J - K$ and redder at $K - L'$ than previously observed T dwarfs. Data analysis using model spectra coupled with knowledge of the well-understood primary implies that for the same surface gravity, Gl 570D is about 160 K cooler than Gl 229B. For an age range of 2–5 Gyr, Gl 570D has an effective temperature in the range 784–824 K, a surface gravity $\log g$ in the range 5.00–5.27 (cm s^{-2}), and a luminosity in the range $(2.88–2.98) \times 10^{-6}\ L_{\odot}$.

Subject headings: stars: abundances — stars: atmospheres — stars: individual (Gliese 570D) — stars: low-mass, brown dwarfs

1. INTRODUCTION

Brown dwarfs with effective temperatures of 1800–3000 K have spectra closely resembling those of red dwarf stars at similar temperatures, and the two types of objects share the same classification scheme, either as M-types in roughly the upper two-thirds of this range or as early L-types in the lower one-third. The later L-types (with $T_{\rm eff}$ below about 1800 K) are solely the domain of brown dwarfs, but the visible and short-wavelength infrared spectra of these objects are a steady continuation of the trends seen in the spectra of early L-types, with alkali metal lines, metal hydride bands, and water vapor bands strengthening with decreasing temperature. As the surface of a brown dwarf cools below approximately 1300–1500 K, however, an important chemical change occurs as methane (CH_4) attains a large abundance at the expense of carbon monoxide (CO). The many strong infrared absorption bands of CH_4 and the disappearance of condensates (which significantly affect the spectra of L-types) below the photosphere substantially alter the spectral appearance of the brown dwarf, the former making it totally unlike any stellar object. Once this happens, it is thought that dramatic changes in the short-wavelength infrared spectrum do not occur again until water vapor begins to condense, at temperatures of about 400 K.

Nakajima et al. (1995) and Oppenheimer et al. (1995) used near-infrared imaging and spectroscopy to discover Gliese 229B, the first brown dwarf for which absorption bands of methane and water dominate the 1–2.5 μm region. Since early 1999, roughly a dozen additional brown dwarfs with 1–2.5 μm spectra similar to Gl 229B have been reported (e.g., Strauss et al. 1999; Burgasser et al. 1999; Cuby et al. 1999; Tsvetanov et al. 2000; Burgasser, Kirkpatrick, & Brown 2001), largely by the Sloan Digital Sky Survey (SDSS) and the Two Micron All Sky Survey (2MASS), and are currently known as T dwarfs. The similarity of these spectra attests to the expected slow evolution of the short-wavelength infrared spectrum of a T dwarf with decreasing temperature, once methane has become the dominant reservoir of carbon. Recently, dwarfs in the L–T transition region near $T_{\rm eff} \sim 1500$ K with detectable CO and CH_4 in the 1.5–2.5 μm region have also been identified (Leggett et al. 2000; Geballe et al. 2001), and absorption by the fundamental band of CH_4 near 3.3 μm has been found in mid to late L-type dwarfs by Noll et al. (2000).

The discovery of brown dwarfs with temperatures much lower than Gl 229B is made difficult by their lower luminosities and the eventual shift with lower temperatures of the bulk of their emissions toward longer wavelengths, where ground-based observations are more difficult. However, a few brown dwarfs found by 2MASS have temperatures and luminosities significantly below those of Gl 229B–type dwarfs. One of these is Gl 570D, discovered by Burgasser et al. (2000) and estimated by them to have an effective temperature of 750 ± 50 K and luminosity of $(2.8 \pm 0.3) \times 10^{-6}\ L_{\odot}$. We have obtained a medium-resolution, 0.8–2.5 μm spectrum of this object, which represents a substantial increase in resolving power, wavelength coverage, and signal-to-noise ratio over that reported by Burgasser et al. (2000). Here we present this spectrum and new photometry, along with a detailed analysis, which yields improved values for temperature, luminosity, and surface gravity.

2. OBSERVATIONS AND DATA REDUCTION

2.1. *Photometry*

JHK infrared photometry was obtained for Gl 570D on UT 2000 February 1 with the UFTI camera on the 3.8 m United Kingdom Infrared Telescope (UKIRT) on Mauna Kea. L' photometry was obtained on 2000 May 15 with IRCAM and also on UKIRT. Weather conditions were photometric on both nights. No color term is needed to convert the L' data to the established UKIRT L' system;

[1] Gemini Observatory, 670 North A'ohoku Place, Hilo, HI 96720; tgeballe@gemini.edu.
[2] Department of Physics and Astronomy, Vanderbilt University, Nashville, TN 37235; dsaumon@cactus.phy.vanderbilt.edu.
[3] Joint Astronomy Centre, 660 North A'ohoku Place, Hilo, HI 96720; s.leggett@jach.hawaii.edu.
[4] Princeton University Observatory, Peyton Hall, Ivy Lane, Princeton, NJ 08544; gk@astro.princeton.edu.
[5] NASA Ames Research Center, Moffett Field, CA 94035; and Department of Astronomy, New Mexico State University, Box 30001, MSC 4500, Las Cruces, NM 88003; mmarley@mail.arc.nasa.gov.
[6] Department of Earth and Planetary Sciences, Washington University, Campus Box 1169, 1 Brookings Drive, St. Louis, MO 63130; lodders@levee.wustl.edu.

TABLE 1

SPECTROSCOPY OF GL 570D

UT Date	Wavelength Range (μm)	Resolution (μm)	Integration Time (s)
2000 Mar 13.....	1.88–2.52	0.0050	2400
	1.43–2.07	0.0050	1920
2000 Mar 14.....	1.03–1.35	0.0025	2880
2000 Mar 15.....	0.79–1.11	0.0025	4800

however, the J, H, and K photometric systems are different from the UKIRT system as a result of significant differences in the filter set. The new photometric system is referred to as the "MKO-NIR" system, as the recently specified Mauna Kea Observatory near-infrared filter set defines the system. Transformations between the established UKIRT system and the new MKO-NIR system are presented by Hawarden et al. (2001).

2.2. *Spectroscopy*

Spectra of Gl 570D were acquired at UKIRT on UT 2000 March 13–15 using the facility's 1–5 μm two-dimensional array spectrometer, CGS4 (Mountain et al. 1990). An observing log is provided in Table 1. Sky conditions were excellent. The observations employed CGS4's 40 line mm^{-1} grating in second order shortward of 1.4 μm and in first order longward of that wavelength, and a 2 pixel (1.″2) wide, 80″ long slit. Observations were obtained in the stare: nod-along-slit mode, with a nod of 7.″32 (corresponding to 12 rows on the array). Prior to observing G1 570D in each wave band, the spectrum of the nearby F5 V star HD 126819 was measured for the purpose of flux calibration and removal of telluric absorption lines. Spectra of argon and krypton arc lamps were obtained for wavelength calibration.

The data reduction employed Figaro routines to extract source spectra from the spectral images produced by the CGS4 array and to wavelength-calibrate them, ratio them, and perform an initial flux calibration. It was found that where the spectral segments overlapped or adjoined one another (at 1.0–1.1, 1.3–1.5, and 1.9–2.1 μm), they did not match perfectly; typical disagreements were 10%. The mismatches are probably due to variations in guiding accuracy and in seeing during the observations, as well as probable inaccuracies in the infrared magnitudes of the calibration star used in the reduction. The spectral segments were scaled by small factors in order to adjoin to one another smoothly and to match the photometry as well as possible, which they do to $\pm 5\%$.

3. RESULTS

Table 2 gives the $JHKL'$ values in the MKO-NIR system as well as in the UKIRT system. The latter have been calculated by convolving the flux-calibrated energy distribution with the old filter profiles. These show Gl 570D to be considerably bluer at $J - K$ than reported by Burgasser et al. (2000), and indeed bluer than all but one T dwarf reported to date. For example, for the T dwarfs Gl 229B, SDSS 1346, and SDSS 1624, $J - K$ is in the range $-0.4 \leq J - K \leq -0.1$ (Leggett et al. 1999, 2000), whereas for Gl 570D, $J - K$ is -0.51 ± 0.07 (both in the UKIRT system). This increasing blueness continues the trend that has been found from the latest L-types, through the earliest T-types, and on to the classical T dwarfs such as Gl 229B (Leggett et al. 2000). Furthermore, Stephens et al. (2001) and Marley et al. (2001) find that $K - L'$ increases monotonically through the L and T sequence. Stephens et al. (2001) find SDSS 1624 to have the reddest $K - L'$ of five T dwarfs observed at 2.54 ± 0.08, while we find that Gl 570D has $K - L' = 3.54 \pm 0.05$, again suggesting that Gl 570D is quite cool.

TABLE 2

NEW PHOTOMETRY OF GL 570D

Band	Magnitude
MKO-NIR:	
J	14.82 ± 0.05
H	15.28 ± 0.05
K	15.52 ± 0.05
L'	12.98 ± 0.05
UKIRT:	
J	15.12
H	15.32
K	15.63

The 0.83–2.52 μm spectrum of Gl 570D (continuous apart from a gap at 1.36–1.44 μm and slightly smoothed) is shown in Figure 1. The figure also contains a spectrum of Gl 229B (Geballe et al. 1996; flux-calibrated by Leggett et al. 1999) for comparison. The only atomic feature observed in the

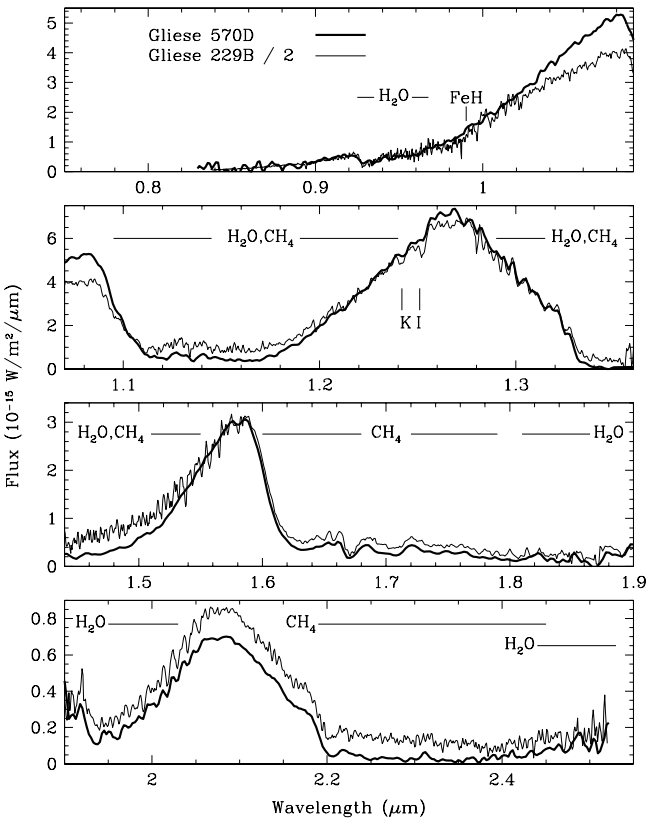

FIG. 1.—Spectrum of Gl 570D (this paper) and Gl 229B (Geballe et al. 1996; Leggett et al. 1999), the latter divided by 2, with principal molecular absorption features and the potassium 1.25 μm doublet identified. The Gl 570D spectrum is slightly smoothed and has resolutions of 0.003 μm shortward of 1.4 μm and 0.006 μm longward of 1.4 μm; those of Gl 229B are 0.0015 and 0.003 μm, respectively.

spectrum of Gl 570D is the potassium doublet near 1.25 μm, which is considerably weaker than the doublet in Gl 229B and is only just discernible. The strong absorption bands of CH_4 and H_2O define the overall shapes of the two spectra, which are quite similar. However, the bands are deeper and in some cases broader in Gl 570D than in Gl 229B. The increasing blueness at $J - K$ with decreasing temperature is thus seen to be a consequence of the relative degrees of strengthening of the (already very strong) absorption bands of water and methane. It is also due in part to the increased opacities of the broad (and blended) H_2 pressure-induced 1–0 $S(1)$, $S(0)$, and $Q(1)$ absorptions at 2.12, 2.22, and 2.41 μm (see, e.g., Borysow, Jørgensen, & Zheng 1996).

4. MODELING OF GLIESE 570D

The following analysis is based on the brown dwarf atmospheric models described by Burrows et al. (1997) and Saumon et al. (2000) and on the 0.8–2.5 μm spectroscopy and photometry presented here. Briefly, the atmospheres are in radiative-convective equilibrium and the molecular opacities are treated with the k-coefficient method (Goody et al. 1989; Lacis & Oinas 1991). Chemical equilibrium is treated as in Burrows et al. (1997). Gas-phase opacities include Rayleigh scattering, the collision-induced opacity of H_2, and the molecular opacities of H_2O, CH_4, NH_3, H_2S, PH_3, CO, VO, and FeH, as well as the continuum opacities of H^- and H_2^-. The present models also include the line opacities of Na, K, and Cs as described in Burrows, Marley, & Sharp (2000). It appears that condensates do not play a significant role in shaping the spectrum of the cooler T dwarfs (Burrows et al. 2000; but see Tsuji, Ohnaka, & Aoki 1999). The opacities of condensation clouds are not included in the present models, although the chemical equilibrium calculation takes into account the formation of condensates. Particulates are assumed to fall below the spectroscopically accessible region of the atmosphere. The equation of radiative transfer is solved, including scattering, following Toon (1989).

Compared with the T dwarf Gl 229B, Gl 570D offers the advantage that the primary star of the system is fairly well studied. The metallicity of Gl 570A was determined by Hearnshaw (1976) and Feltzing & Gustafsson (1998) to be [Fe/H] = 0.01 and 0.00 $\pm$ 0.12, respectively. We adopt the solar abundances of Anders & Grevesse (1989) for modeling Gl 570D.

Using the same monochromatic opacities used to compute the k-coefficients, high-resolution synthetic spectra were generated from the atmospheric structures by solving the radiative transfer equation with the Feautrier method (Mihalas 1978) on a frequency grid with $\Delta\nu = 1$ cm^{-1}. The synthetic spectra were convolved with a Gaussian filter to match the resolution of the observations.

4.1. *Luminosity, Effective Temperature, and Gravity*

Because the present spectrum samples more than half of the flux emitted by Gl 570D, and because the distance is known to be 5.91 $\pm$ 0.06 pc (Perryman et al. 1997), we can tightly constrain the possible solutions for the surface parameters of Gl 570D by using both synthetic spectra and evolution calculations. We use a method similar to the one applied to Gl 229B by Saumon et al. (2000). The solar-metallicity evolution sequence for cooling brown dwarfs of Burrows et al. (1997) specifies uniquely the bolometric luminosity $L_{\rm bol}$ of a brown dwarf in terms of the effective temperature $T_{\rm eff}$ and the surface gravity g. This defines a surface $L_{\rm bol}(T_{\rm eff}, g)$.

Our spectrum samples the energy distribution of Gl 570D from 0.83 to 2.52 μm. The integral of the observed flux over wavelength, $L_s = 1.581 \times 10^{-15}$ W m^{-2}, allows us to estimate $L_{\rm bol}$. We obtain the bolometric correction factor from our synthetic spectra by taking the ratio of the flux integrated over the observed wavelength range to the total emergent flux ($\sigma T_{\rm eff}^4$). This synthetic correction is a function of the spectrum parameters, $T_{\rm eff}$ and g, and is found to vary between 1.6 and 1.9 in the parameter range of interest here. By applying the bolometric correction to the empirically determined flux, we obtain another relation for the bolometric luminosity, $L_{\rm bol}(T_{\rm eff}, g)$. The intersection of the two $L_{\rm bol}$ surfaces gives a curve $T_{\rm eff}(g)$, which represents the allowed parameters for Gl 570D. For a given gravity, this curve and the cooling sequence give $T_{\rm eff}$, $L_{\rm bol}$, the mass, the radius, and the age of the brown dwarf. The results are given in Table 3 for three representative gravities.

There are three sources of uncertainty in our determination of $L_{\rm bol}$. The distance to Gl 570D is known to a precision of $\pm$1%, and the absolute calibration of our spectrum has an uncertainty of $\pm$5%. Finally, the synthetic bolometric correction depends on the reliability of our synthetic spectra. As discussed below (see § 4.2), there are systematic differences between the synthetic and observed spectra of T dwarfs. Fortunately, these tend to cancel out when calculating integrated fluxes for the bolometric correction. For example, varying the abundance of the main absorber, H_2O, by 0.1 dex affects the bolometric correction by only 2%. A consistency check can be made with the L' measurement, which we did not include in the computation of the bolometric correction. The synthetic L' magnitude is 14.32, or 0.2 mag fainter than the observed value. However, only 7.6% of the total flux of Gl 570D is in the L' band, so the resulting error in the bolometric correction is $\sim$1.5%. Other modifications of the synthetic spectrum calculations all indicate that the bolometric correction is correct to within $\pm$2%. The uncertainties in $L_{\rm bol}$ and $T_{\rm eff}$ are thus $\pm$6% ($\pm$0.03 dex) and $\pm$12 K, respectively.

Figure 2 shows the models listed in Table 3 superposed on brown dwarf cooling curves. The nearly vertical band running through the center is a constant-luminosity curve with the luminosity of model B [$\log(L/L_\odot) = -5.526 \pm 0.03$]. Since all three models A, B, and C have nearly the same luminosity (see Table 3), models A and C also fall within that band. We find that for a given, assumed gravity, Gl 570D is about 160 K cooler than Gl 229B.

4.1.1. *Age of the Gl 570 System*

So far, we have greatly reduced the allowed space for the physical parameters of Gl 570D (see Fig. 2). However, while $T_{\rm eff}$ is between 700 and 870 K, and the well-determined luminosity can range from $\log(L/L_\odot) = -5.55$ to -5.50, the gravity remains largely unconstrained and with it, the

TABLE 3

PHYSICAL PARAMETERS AS A FUNCTION OF SURFACE GRAVITY

Model	$\log g$ (cgs)	$T_{\rm eff}$ (K)	$\log(L/L_\odot)$	Mass (M_J)	Radius ($R_\odot$)	Age (Gyr)
A.....	4.5	734	−5.503	15	0.1095	0.4
B.....	5.0	784	−5.526	34	0.0935	2
C.....	5.5	854	−5.551	72	0.0776	10

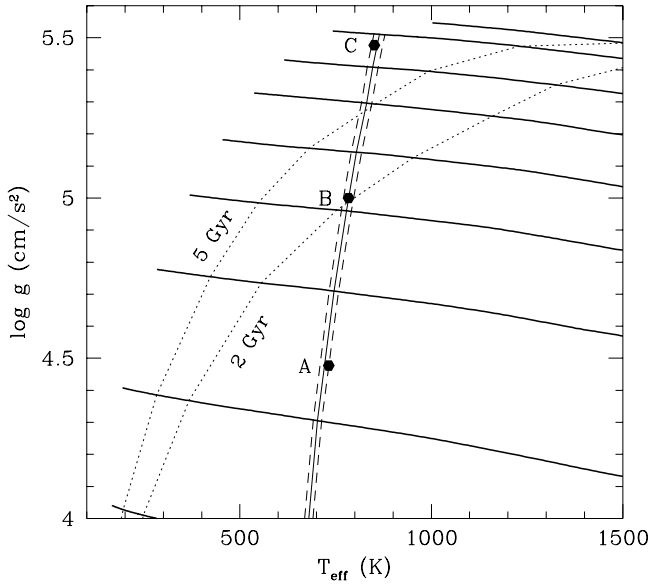

FIG. 2.—Evolution of solar-metallicity brown dwarfs and giant planets in effective temperature–gravity space. The heavy solid lines are cooling tracks for objects with masses of 0.075, 0.07, 0.06, 0.05, 0.04, 0.03, 0.02, and 0.01 $M_\odot$, from top to bottom, respectively (Burrows et al. 1997). Evolution proceeds from right to left; the isochrones bracketing the age of Gl 570D are shown by dotted lines. The band crossing the center of the figure is the locus of all models with the luminosity of Gl 570D model B. Filled symbols correspond to the models listed in Table 3 and used for the present analysis.

mass and age of Gl 570D. We can reduce the possible range of gravities by determining the age of the system. Fortunately, the primary star, Gl 570A, is a well-observed K4 V star to which we can apply several age indicators. The Gl 570 system contains a spectroscopic binary, Gl 570BC. Based on the projected separation of the A-BC system (147 AU), the mass of the primary ($\sim$0.7 $M_\odot$), and the mass of the BC pair (0.976 $M_\odot$), the orbital period of the A-BC system is on the order of 1400 yr (Forveille et al. 1999). By comparison, the rotation period of Gl 570A is only 40 days (Cumming, Marcy, & Butler 1999). We can safely assume that there has been no spin-up of the primary star due to tidal interaction with the BC pair, and that we can use stellar activity indicators as if Gl 570A were an isolated star.

The X-ray luminosity of Gl 570A is $\log L_X(\mathrm{ergs\ s^{-1}}) = 27.72$, or $\sim$5 times lower than stars in the Hyades of the same spectral type (Stern, Schmitt, & Kahabka 1995), clearly indicating that Gl 570A is older than the Hyades cluster. Gl 570A has old disk kinematics (Leggett 1992) and thus is older than $\sim$1.5 Gyr (Eggen 1989). The BC pair has a combined spectral type of M1 V, with individual masses of 0.586 and 0.390 $M_\odot$, respectively (Forveille et al. 1999). The lack of Hα emission from the BC pair indicates that it is older than $\sim$2 Gyr (Soderblom, Duncan, & Johnson 1991; Hawley, Gizis, & Reid 1996). Thus these indicators suggest a lower bound of $\sim$2 Gyr for the age of the Gl 570 system.

On the other hand, Gl 570A is chromospherically active with a Ca II H and K emission index of $\log R'_{HK} = -4.49$ (Henry et al. 1996). This is 0.15 less than stars in the Hyades of the same spectral type, indicating that Gl 570A is older than the Hyades, in complete agreement with our lower bound for the age. For comparison, the Sun varies from $\log R'_{HK} = -5.10$ to -4.75 during the solar cycle and is considered inactive. Using the age–emission index relation of Donahue (1993; given in Henry et al. 1996), we obtain an age of 0.8 Gyr for Gl 570A. However, if we assume that Gl 570A was observed during a maximum phase of activity and that its emission index varies with the same amplitude as the Sun's, then the emission index of Gl 570A might be as low as $\log R'_{HK} = -4.84$, with a corresponding age of 3.1 Gyr. Figure 10 of Soderblom et al. (1991) shows the data used to derive a similar age–emission index relation. If we consider the stars showing the most extreme scatter toward older ages for a given value of $\log R'_{HK}$, including the error bars on the age determinations, we find that to be older than the Sun, Gl 570A would have to have an emission index of less than -4.95, which is extremely unlikely. We conclude that the chromospheric activity of Gl 570A indicates relative youth and a very conservative upper bound of 5 Gyr for its age.

4.1.2. *Optimal Parameters*

Figure 2 shows isochrones for our adopted age range for the Gl 570 system. The allowed range of gravities for Gl 570D is now considerably reduced, to $5.00 \leq \log g\ (\mathrm{cm\ s^{-2}}) \leq 5.27$. These extremes correspond to $T_{\rm eff} = 784$ (824) K, $\log (L/L_\odot) = -5.53$ (-5.54), and $M = 34$ (52) M_J, respectively. Our values for the physical parameters of Gl 570D agree very well with the estimates of Burgasser et al. (2000). The midpoints of these ranges are $\log g = 5.13$, $T_{\rm eff} = 804 \pm 12$ K, and $L = (2.93 \pm 0.18) \times 10^{-6}\ L_\odot$. The last is less than half the luminosity of Gl 229B. A meaningful comparison of the masses of Gl 570D and Gl 229B is not possible, since the mass of the latter is poorly constrained.

We derived the physical parameters simply from the observed integrated flux, the distance to Gl 570D, synthetic bolometric corrections, and cooling tracks for brown dwarfs. As for Gl 229B (Saumon et al. 2000), it was not necessary to fit the observed spectrum with models to derive $T_{\rm eff}$ and the gravity. While the synthetic spectra of T dwarfs are fairly successful at reproducing the observations, there are known problems that affect a few spectral regions (see § 4.2 below). Fitting the spectrum over a wide range of wavelengths remains an imprecise exercise, and our method is far more reliable. By relying only on wavelength-integrated fluxes, most of the errors in the synthetic spectrum cancel one another. Our procedure also uses cooling calculations for the $L(T_{\rm eff}, g)$ relation, which is rather insensitive to the details of the atmospheric surface boundary condition. Further improvements in the modeling of brown dwarf atmospheres, principally by the inclusion of condensation clouds, will have a very modest effect on this relation.

4.2. *Synthetic Spectrum*

We have computed synthetic spectra for the models in Table 3. The flux received at Earth is simply obtained from the radius of each model and the distance to Gl 570D. The resulting spectra are compared with our 0.83–2.52 μm spectrum in Figure 3. We emphasize that no fitting of the spectra has been performed, although spectrum B is generally a better fit to the observations than either A or C. The overall agreement of the model with the data is remarkable. This demonstrates both the power and the internal consistency of our method of analysis and that the overall spectral energy distribution is well modeled. Nevertheless, all three models show particular deviations from the observed spectrum, most of which are also seen in models for Gl 229B (Allard et al. 1996; Marley et al. 1996; Saumon et al. 2000).

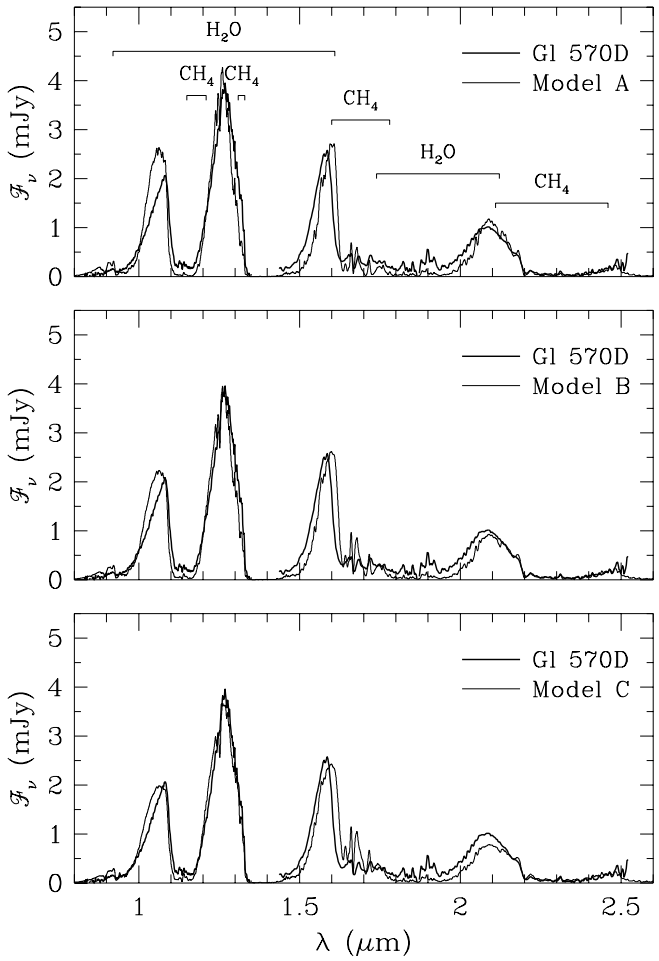

FIG. 3.—Comparison of synthetic and observed spectra for each of the models shown in Fig. 2. The synthetic fluxes are not normalized to the data but obtained from the radius of each model (see Table 3) and the distance of the Gl 570 system. The molecules responsible for the spectral features in each region are identified in the top panel.

As discussed by Saumon et al. (2000), the CH_4 opacity line list becomes increasingly incomplete at temperatures above 300 K. Since Gl 570D is about 160 K cooler than Gl 229B, we expect to obtain a better agreement with the observed spectrum in the CH_4 bands. Indeed, the 2.3 μm CH_4 band, which is formed at a level where $T \sim 600$ K, matches the data extremely well. The 1.6 μm band is formed at $T \sim 800$ K, and its overall strength also matches well. However, the edge of the band appears at longer wavelengths in the model, and the features in the 1.63–1.72 μm region have a much larger amplitude than in the data. This also occurs in models of Gl 229B and shows the limitation of the CH_4 opacity database.

The H_2O bands in the model are too strong, notably in the 1.1–1.2, 1.3–1.6, and 1.8–2.1 μm regions. This problem has also plagued cloudless models of Gl 229B and cannot be resolved by simply invoking a lower abundance of H_2O. Its persistence suggests that condensates are present in the atmosphere (Tsuji et al. 1999; Ackerman & Marley 2001), and that they have a small but detectable effect on the spectrum.

The heavily pressure-broadened K I resonance doublet at 0.77 μm is mostly responsible for the very weak flux at 0.8–1.0 μm (Tsuji et al. 1999; Burrows et al. 2000). In this model, the opacity of the doublet is significant up to 1.1 μm, yet the flux is overestimated on the blue side of the 1.08 μm peak. Most of this mismatch is due to an underabundance of neutral K in the cooler part of the atmosphere.

The potassium abundance at levels where $T \lesssim 1400$ K depends on the overall treatment of condensates and can be modeled in two ways. One is to consider that condensates form and remain in local equilibrium with the gas. This means that existing high-temperature (primary) condensates can react with the gas at lower temperatures, and that secondary condensates form via gas-solid reactions in the upper, cooler part of the atmosphere. This is the case described as "no rainout" by Burrows & Sharp (1999) and Burrows et al. (2000) and is the one used in the present analysis. However, this scenario for condensate formation may be relevant only for low-gravity environments such as the solar nebula and stellar outflows and thus may be unlikely for brown dwarf atmospheres.

A second approach to condensate formation, more appropriate to low-mass stars and brown dwarfs, is the "condensation cloud formation" model, also described as "rainout" by Burrows & Sharp (1999) and Burrows et al. (2000). Primary condensates form directly from the gas and are sequestered in a condensate cloud of finite vertical extent because of the gravity field. This prevents the formation of secondary condensates by gas-solid reactions at lower temperatures (above the cloud) that deplete the abundance of gaseous potassium in the former case of no rainout. The condensation cloud formation model predicts a higher abundance of gaseous potassium in the upper part of the atmospheres of T dwarfs (compare Figs. 2 and 3 of Burrows et al. 2000). In Figure 4, we compare the spectrum computed with the K I abundance from our calculation without rainout (*light solid curve*; Burrows & Sharp 1999) and with the condensation cloud formation model (*dotted curve*; Lodders 1999). The latter agrees much better with the observed spectrum in the region dominated by the K I reso-

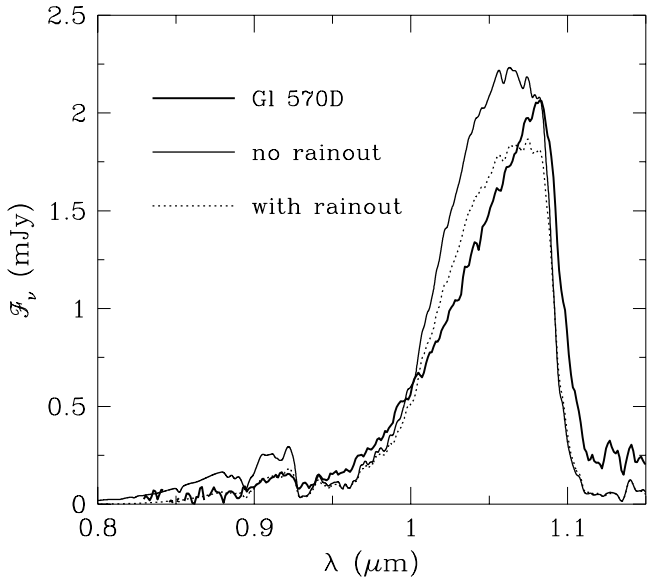

FIG. 4.—Two spectra computed from model B under different assumptions for the computation of chemical equilibrium; i.e., that condensates do and do not rainout of the atmosphere. In the former case, the K I abundance is higher in the upper reaches of the atmosphere, and a better fit to the observed spectrum shortward of 1.1 μm is obtained.

nance doublet. This further strengthens the case for the formation of condensate clouds in the atmospheres of T dwarfs as argued by Fegley & Lodders (1996) and Lodders (1999).

The K I doublet at 1.2432 and 1.2522 μm is weak but detected in our spectrum, while the model predicts very strong lines. Decreasing $T_{\rm eff}$, increasing g, and decreasing the potassium abundance could all reduce the strength of the lines in the model. The magnitude of the changes required in these parameters is unreasonable in view of the other constraints, however. The two lines of the doublet share the same lower level of K I (about 1.6 eV above the ground state) and are quite sensitive to temperature. In Gl 570D, this doublet is formed at the level where $T \sim 1600$ K. The strength of the doublet decreases rapidly at lower temperatures. The larger than observed strength of the computed K I doublet may be due to remaining uncertainties in the (T, P)-profile in the atmosphere model (perhaps due to the effects of condensates deep in the atmosphere). If this is the case, the 1.25 μm doublet of K I could become a powerful probe of the temperature profile in T dwarf atmospheres.

A better fit to the spectrum of Gl 570D could be obtained with a more detailed study. While the deviations we find could be due to residual uncertainties in the (T, P)-profile of the atmosphere or the presence of a warm dust layer, compositional variations from a solar mixture of heavy elements may play a role. Feltzing & Gustafsson (1998) found that the abundances of individual elements in Gl 570A are scattered around the solar values by ± 0.4 dex. In particular, they find [O/H] = 0.16, [Na/H] = 0.06, and [Ca/H] = -0.11] with uncertainties of ± 0.1–0.2 dex. If the abundances of several other key elements (C, N, O, K, Si, and Mg, for example) also deviate appreciably from their solar values, and if we assume that Gl 570D shares the same atmospheric composition as the primary star, the modeled spectrum would be altered. Such refinements go beyond the scope of the present study.

5. SUMMARY

New and improved spectra and photometry of Gl 570D, one of the coolest and least-luminous brown dwarfs known, have been analyzed by spectral modeling to yield more accurate estimates of luminosity, effective temperature, and surface gravity. The observations demonstrate that the increasing blueness at $J - K$ of T dwarfs with decreasing temperature continues down to objects with effective temperatures of at least 800 K. Comparison of model spectra with the observed spectra provides some evidence for rainout of condensates and suggests that the K I doublet at 1.25 μm may be a sensitive indicator of the temperature profile in T dwarfs.

We thank A. Burrows for sharing his table of alkali metal abundances, R. A. Donahue for a useful discussion, J. W. Liebert for an important suggestion, and an anonymous referee for several helpful comments. T. R. G.'s research was supported by the Gemini Observatory, which is operated by the Association of Universities for Research in Astronomy, Inc., under a cooperative agreement with the NSF on behalf of the Gemini partnership: the National Science Foundation (US), the Particle Physics and Astronomy Research Council (UK), the National Research Council (Canada), the Australian Research Council (Australia), CNPq (Brazil), and CONICET (Argentina). D. S. acknowledges support from NASA through grant NAG 5-4988. G. R. K. thanks NASA for support via grant NSG 5-6734. Work by K. L. was supported by NSF grant AST 00-86487. Work by M. S. M. was supported by NSF CAREER grant AST 96-24878 and NASA grant NAG 5-8919. The United Kingdom Infrared Telescope is operated by the Joint Astronomy Centre on behalf of the UK Particle Physics and Astronomy Research Council. We thank the staff of UKIRT for its support of these observations and the UKIRT Service Program for providing the L' photometry.

REFERENCES

Ackerman, A., & Marley, M. 2001, ApJ, in press
Allard, F., Hauschildt, P. H., Baraffe, I., & Chabrier, G. 1996, ApJ, 465, L123
Anders, E., & Grevesse, N. 1989, Geochim. Cosmochim. Acta, 53, 197
Borysow, A., Jørgensen, U. G., & Zheng, C. 1997, A&A, 324, 185
Burgasser, A. J., Kirkpatrick, D., & Brown, M. E. 2001, in Proc. Ultracool Dwarfs Workshop, ed. H. R. A. Jones, M. Gerbaldi, & I. A. Steele (Heidelberg: Springer), in press
Burgasser, A. J., et al. 1999, ApJ, 522, L65
———. 2000, ApJ, 531, L57
Burrows, A., et al. 1997, ApJ, 491, 856
Burrows, A., Marley, M. S., & Sharp, C. M. 2000, ApJ, 531, 438
Burrows, A., & Sharp, C. M. 1999, ApJ, 512, 843
Cuby, J. G., Saracco, P., Moorwood, A. F. M., D'Odorico, S., Lidman, C., Comeron, F., & Spyromilio, J. 1999, A&A, 349, L41
Cumming, A., Marcy, G. W., & Butler, R. P. 1999, ApJ, 526, 890
Donahue, R. A. 1993, Ph.D. thesis, New Mexico State Univ.
Eggen, O. J. 1989, PASP, 101, 366
Fegley, B., Jr., & Lodders, K. 1996, ApJ, 472, L37
Feltzing, S., & Gustafsson, B. 1998, A&AS, 129, 237
Forveille, T., et al. 1999, A&A, 351, 619
Geballe, T. R., Kulkarni, S. R., Woodward, C. E., & Sloan, G. C. 1996, ApJ, 467, L101
Geballe, T. R., et al. 2001, ApJ, submitted
Goody, R., West, R., Chen, L., & Crisp, D. 1989, J. Quant. Spectrosc. Radiat. Transfer, 42, 539
Hawarden, T. G., Leggett, S. K., Letawsky, M. B., Ballantyne, D. R., & Casali, M. M. 2001, MNRAS, in press
Hawley, S. L., Gizis, J. E., & Reid, I. N. 1996, AJ, 112, 2799
Hearnshaw, J. B. 1976, A&A, 51, 85
Henry, T. J., Soderblom, D. R., Donahue, R. A., & Baliunas, S. L. 1996, AJ, 111, 439
Lacis, A. A., & Oinas, V. 1991, J. Geophys. Res., 96, 9027
Leggett, S. K. 1992, ApJS, 82, 351
Leggett, S. K., et al. 2000, ApJ, 536, L35
Leggett, S. K., Toomey, D. W., Geballe, T. R., & Brown, R. H. 1999, ApJ, 517, L139
Lodders, K. 1999, ApJ, 519, 793
Marley, M. S., Saumon, D., Guillot, T., Freedman, R. S., Hubbard, W. B., Burrows, A., & Lunine, J. I. 1996, Science, 272, 1919
Marley, M. S., Seager, S., Saumon, D., Lodders, K., Ackerman, A. S., & Freedman, R. 2001, ApJ, submitted
Mihalas, D. 1978, Stellar Atmospheres (2d ed.; San Francisco: Freeman)
Mountain, C. M., Robertson, D., Lee, T. J., & Wade, R. 1990, Proc. SPIE, 1235, 25
Nakajima, T., Oppenheimer, B. R., Kulkarni, S. R., Golimowski, D. A., Matthews, K., & Durrance, S. T. 1995, Nature, 378, 463
Noll, K. S., Geballe, T. R., Leggett, S. K., & Marley, M. S. 2000, ApJ, 541, L75
Oppenheimer, B. R., Kulkarni, S. R., Matthews, K., & Nakajima, T. 1995, Science, 270, 1478
Perryman, M. A. C., et al. 1997, A&A, 323, L49
Saumon, D., Geballe, T. R., Leggett, S. K., Marley, M. S., Freedman, R. S., Lodders, K., Fegley, B., Jr., & Sengupta, S. K. 2000, ApJ, 541, 374
Soderblom, D. R., Duncan, D. K., & Johnson, D. R. H. 1991, ApJ, 375, 722
Stephens, D., Marley, M., Noll, K., & Chanover, N. 2001, ApJL, submitted

Stern, R. A., Schmitt, J. H. M. M., & Kahabka, P. T. 1995, ApJ, 448, 683
Strauss, M. A., et al. 1999, ApJ, 522, L61
Toon, O. B., McKay, C. P., Ackerman, T. P., & Santhanam, K. 1989, J. Geophys. Res., 94, 16287
Tsuji, T., Ohnaka, K., & Aoki, W. 1999, ApJ, 520, L119
Tsvetanov, Z. I., et al. 2000, ApJ, 531, L61